

ARTICLE

Desulfurization Mechanism of Cysteine in Synthesis of Polypeptides

Yan Tian^{a,b}, Li Wang^a, Jing Shi^{b*}, Hai-zhu Yu^{c*}*a. Department of Applied Chemistry, Anhui Agricultural University, Hefei 230036, China**b. Department of Chemistry, University of Science and Technology of China, Hefei 230026, China**c. Department of Chemistry and Centre for Atomic Engineering of Advanced Materials, Anhui University, Hefei 230601, China*

(Dated: Received on January 23, 2015; Accepted on March 28, 2015)

The free-radical-based selective desulfurization of cysteine residue is an efficient protocol to achieve ligations at alanine sites in the synthesis of polypeptide and proteins. In this work, the mechanism of desulfurization process has been studied using the density functional theory methods. According to the calculation results, the desulfurization of the thiol group occurs via a three-steps mechanism: the abstraction of hydrogen atom on the thiol group with the radical initiator VA-044 (2,2'-azobis[2-(2-imidazolin-2-yl)propane]dihydrochloride), the removal of S atom under the reductant TCEP (tris(2-carboxyethyl)phosphine), and the formation of RH molecule (with the regeneration of RS radical). The second step (desulfurization step) is the rate-determining step, and the adduct *t*-BuSH facilitates the desulfurization of cysteine via benefiting the formation of the precursor of the desulfurization step.

Key words: Cysteine, Desulfurization, Reaction mechanism, Density functional theory

I. INTRODUCTION

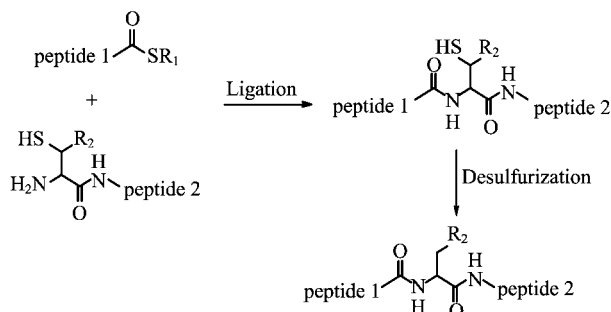
As the elementary motif in multiple polypeptide chains, peptide has been frequently used in preparing polypeptides via biological and chemical synthetic methods. So far, one of the most powerful approaches is the native chemical ligation (NCL) developed by Kent and co-workers [1]. NCL corresponds to a chemoselective reaction between an N-terminal cysteine (Cys) residue and a C-terminal thioester under neutral pH conditions, and produces an elongated polypeptide with an amide bond at the ligation point. Due to its chemoselectivity, ease of operation and high efficiency, NCL has been widely used in chemical total synthesis and semi-synthesis of proteins [2, 3]. Nonetheless, the necessity for the N-terminal Cys residue at the ligation site significantly limits its application.

In the past decades, considerable efforts have been made to improve the NCL method [4]. One of the most effective strategies is the ligation-desulfurization approach. In this approach, a thiol group is first attached to the *N*-terminal amino acid, and then reacts with C-terminal peptide thioester by native chemical ligation process. After ligation, the thiol group can be chemically removed to achieve ligations at non-cysteine sites (Scheme 1). This protocol greatly expands the scope of

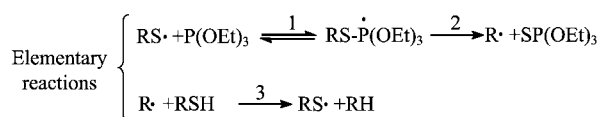
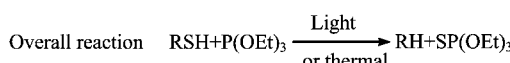
NCL methods. For example, Dawson *et al.* proposed that either Raney nickel or Pd/Al₂O₃ can be used to desulfurize cysteine to achieve ligations at alanine sites [5]. Similarly, the metal-catalyzed desulfurization approach has been successfully employed in the synthesis of some non-cysteine proteins and cyclic peptides [6]. However, this method always suffers from low yields and excessive demand for nickel reagent [7]. In addition, the Raney nickel is not compatible with the extensive functionality present in glycopeptide substrate systems, and causes the reduction of thiol/thioether [8]. The epimerization of the secondary alcohols might also occur in the presence of metal reducing reagent [9]. To settle these problems, Danishefsky group recently developed a free-radical based desulfurization approach [10]. In this method, the water-soluble 2,2'-azobis[2-(2-imidazolin-2-yl)propane] dihydrochloride (VA-044) was used as the radical initiator and tris(2-carboxyethyl)phosphine (TCEP) was used as the reducing reagent. Meanwhile, *t*-BuSH added in all the desulfurization processes. With this strategy, the concerned Cys residue in different peptides could be converted to Ala in good yields (70%–90%) at low temperatures (room temperature or 37 °C), implying the great potential of this method in the synthesis of glycopeptide and polypeptides [11, 12].

As to the mechanism of desulfurization, Rabinowitz previously proposed a mechanism for P(OEt)₃ mediated desulfurization of thiol group (Scheme 2) [13]. The first step involves a reversible addition of alkylthiyl radical to phosphite, which generates a phosphoranyl radical intermediate. Subsequently, the β -elimination of phosphoranyl radical generates an alkyl radical (step

* Authors to whom correspondence should be addressed. E-mail: 18611451229@163.com, shijing@ustc.edu.cn, Tel.: +86-551-6360476, FAX: +86-551-63606689



Scheme 1 The ligation-desulfurization approach.



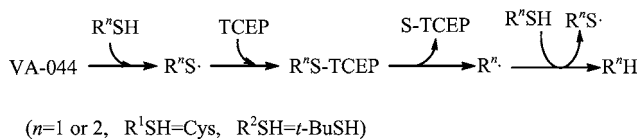
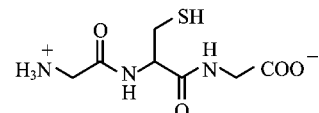
Scheme 2 Proposed mechanism of radical desulfurization reaction [13].

2). Finally, the alkyl radical rapidly abstracts hydrogen atom from the parent thiol and yields the alkane product. Similar to Rabinowitz's proposal, Danishefsky *et al.* [10] suggested that the desulfurization mechanism of cysteine molecule (R^1SH) or the adduct $t\text{-BuSH}$ (R^2SH) might occur via the following three steps (Scheme 3): the abstraction of hydrogen atom of R^nSH with the radical initiator VA-044, the removal of S atom under the reductant TCEP, and the formation of RH molecule (with the regeneration of R^nS radical).

Despite the aforementioned mechanism (Scheme 3), some of the intrinsic details remain ambiguous. For example, the detailed energetics and structures of the intermediates and transition states involved in these steps remains unknown. Meanwhile, the rate-determining step of the desulfurization and the effect of $t\text{-BuSH}$ are also needed to be clarified. To solve these problems, we performed density functional theory (DFT) calculations on the desulfurization of Cys residue reported by Danishefsky *et al.* [10]. We hope that the calculated results and the related conclusions can provide a better understanding for the desulfurization processes, and benefit the future development of more desulfurization reactions.

II. COMPUTATIONAL DETAILS

All calculations were carried out with Gaussian 09 program [14]. The geometries of all species were optimized using B3LYP method with 6-31+G(d) basis set. Frequency calculations were performed at the same level

Scheme 3 Overall desulfurization mechanism of cysteine with $t\text{-BuSH}$ [10].Scheme 4 Modeling dipeptide R^3SH .

to confirm the stationary points as real minima or transition states. Intrinsic reaction coordinate (IRC) [15] calculations were conducted to confirm that the transition state connects the correct reactant and product on the potential energy surface. Single-point energy calculations were performed on the stationary points by M06-2X [16] method with the 6-31G(d) basis set. In this work, the reported energies were the single-point energies corrected by Gibbs free energy corrections. For all the species, only the most favored conformations were reported and discussed in the following text.

Cys (R^1SH) molecule was first used as the reactant to study the detailed mechanism of the desulfurization process in the gas phase. Thereafter, in accordance with Danishefsky's experiments, a modeling dipeptide R^3SH (Scheme 4) was used to discuss the desulfurization mechanism in water with M06-2X/6-31G(d)/B3LYP/6-31+G(d) method. SMD model was used for the solution-phase single point energy calculations [17].

III. RESULTS AND DISCUSSION

A. Initiation of free radical

As a novel water-soluble azo-type initiator, VA-044 has been widely used due to its high efficiency, robustness, and easy operation [18, 19]. In the initiation step, VA-044 is decomposed into two radicals (A) and N_2 by breaking the double C–N bonds (Scheme 5) [19]. Subsequently, the active radical A can react with either the model reactant Cys (R^1SH) or the adduct $t\text{-BuSH}$ (R^2SH) to generate the radical $\text{RS} \cdot$. In the following section, the two different processes will be discussed respectively.

B. Desulfurization of Cys molecule

The free energy profile of the desulfurization of cysteine molecule (R^1SH) is shown in Fig.1. The radi-

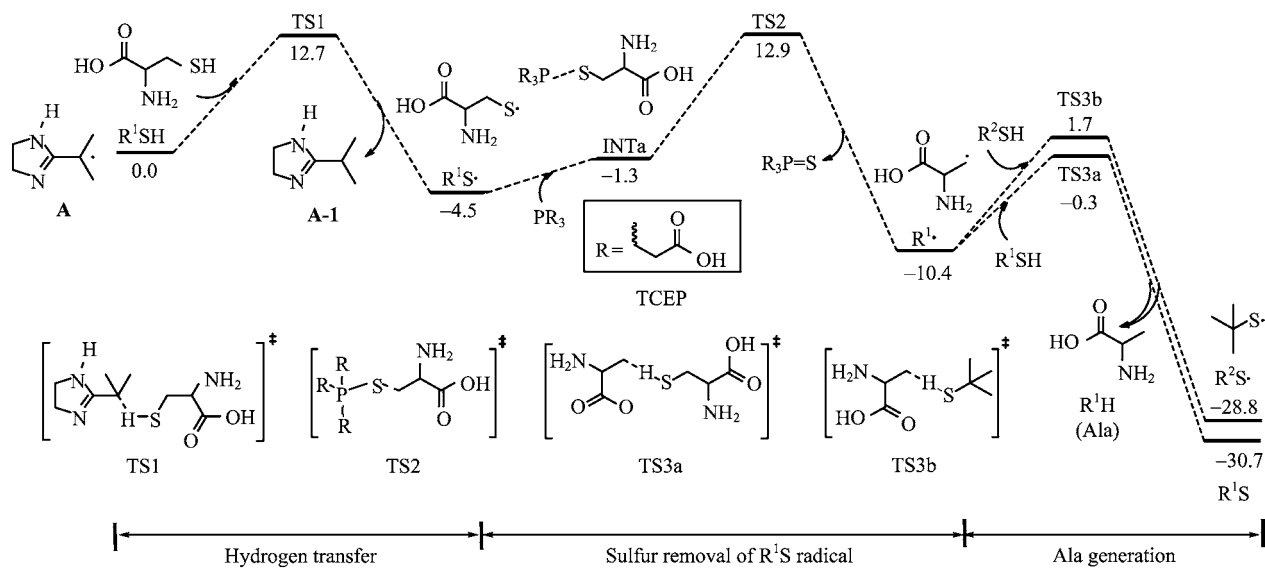
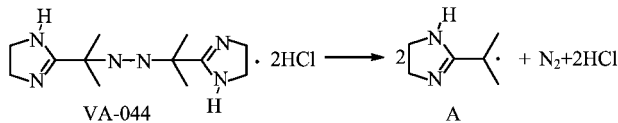


FIG. 1 Free energy profile of the desulfurization of cysteine molecule (in kcal/mol).



Scheme 5 The dissociation of VA-044.

cal center in A first attacks the thiol hydrogen atom of R^1SH via the hydrogen-transfer transition state TS1, and forms the thermodynamically more stable molecule A-1 and the radical $\text{R}^1\text{S}\cdot$. The energy barrier of this hydrogen-transfer step is 12.7 kcal/mol, and the formation of $\text{R}^1\text{S}\cdot$ and A-1 is exergonic by 4.5 kcal/mol. The optimized structure of TS1 in Fig.2 indicates that the breaking S–H bond is lengthened to 1.544 Å, while the distance of forming C–H bond is shortened to 1.477 Å.

Once the radical $\text{R}^1\text{S}\cdot$ is formed, it takes part in the desulfurization cycle by reacting with the reducing reagent TCEP rapidly. Because of the stability and the specificity in reduction of bivalent sulfur, TCEP has been widely used in biochemistry [20]. As shown in Fig.1, the sulfur atom of radical $\text{R}^1\text{S}\cdot$ first attacks the electron-rich phosphorus atom of TCEP to form a tetracoordinated phosphoranyl radical intermediate INTa. This process is endergonic by 3.2 kcal/mol. Herein, it's noteworthy that the relative free energies of the intermediate INTa and the reactant (R^1SH and TCEP) are comparable, implying that the formation of INTa is thermodynamically reversible at room temperature. Subsequently, β -elimination of the intermediate INTa occurs by shortening the S–P bond distance and stretching the C–S bond. The phosphonic compound $\text{R}_3\text{P}=\text{S}$ and radical $\text{R}^1\cdot$ are then formed via the transition state TS2 with a barrier height of 17.4 kcal/mol.

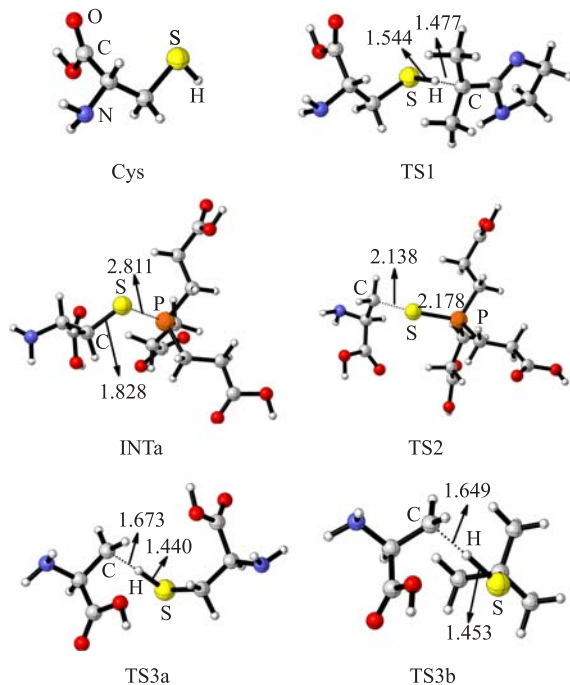


FIG. 2 Optimized geometries of species in the desulfurization process of cysteine molecule. Bond length is in Å.

From optimized structures in β -elimination step (Fig.2), we can see that the C–S and S–P distances in INTa are 1.828 and 2.811 Å, respectively. In TS2, the related bond distances are 2.138 and 2.178 Å, respectively. These values indicate that the S–P bond is gradually strengthened with the simultaneous C–S bond weakening. From $\text{R}^1\cdot$, either R^1SH or R^2SH might partic-

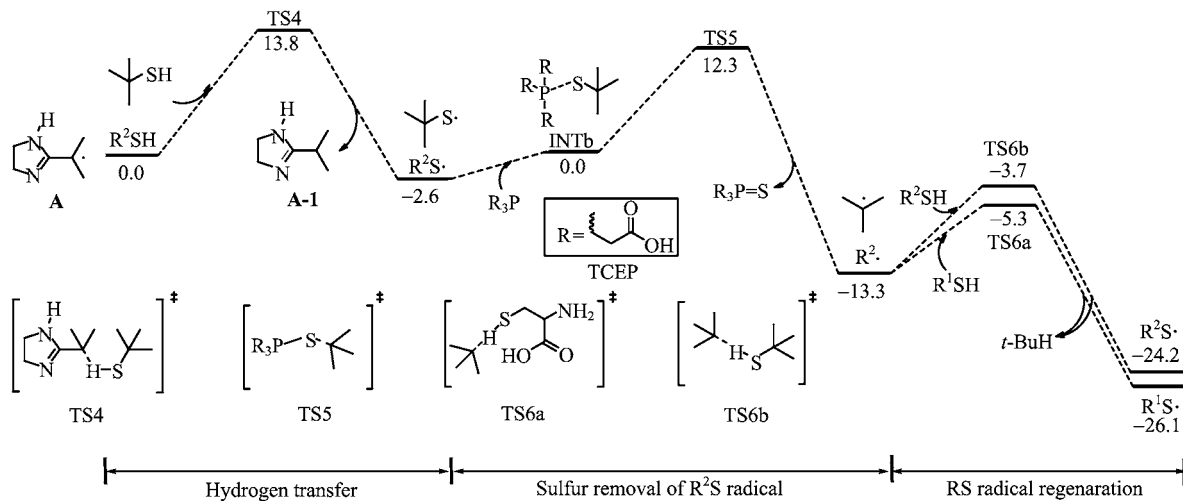


FIG. 3 Free energy profiles of the desulfurization of *t*-BuSH molecule (in kcal/mol).

ipate in the Ala generation step by donating the hydrogen atom to $R^1\cdot$. The calculated energy barriers of the two processes (with R^1SH or R^2SH) are 10.1 and 12.1 kcal/mol, respectively. Meanwhile, the formation of the $R^1S\cdot$ is slightly more exergonic by that of $R^2S\cdot$ (20.3 kcal/mol vs. 18.4 kcal/mol). Accordingly, the hydrogen transfer process of cysteine molecule (R^1SH) is more favorable than that of *t*-BuSH (R^2SH) from both kinetic and thermodynamic aspects. Note that the low energy barrier and the high energy release in this Ala generation step are consistent with Rabinowitz's previous proposal that the formed radical $R^1\cdot$ can rapidly capture the hydrogen atom of thiol [13].

According to the energy profile (Fig.1), the rate-limiting step of the desulfurization of Cys is the second step, *i.e.* sulfur atom removal step. The overall activation energy barrier is 17.4 kcal/mol ($R^1S\cdot \rightarrow TS4$).

C. Desulfurization of *t*-BuSH molecule

To elucidate the effect of *t*-BuSH used in Danishefsky's study, we also examined the desulfurization mechanism starting from *t*-BuSH (R^2SH). Similar to the above discussions starting from R^1SH , the desulfurization of *t*-BuSH molecule also includes three steps (Fig.3). The first step is the hydrogen-abstraction process. Then the radical $R^2S\cdot$ is formed via the hydrogen-transfer transition state TS4. The corresponding energy barrier is 13.8 kcal/mol.

The second step is the reduction of radical $R^2S\cdot$. The sulfur atom of radical $R^2S\cdot$ gradually gets close to the phosphorus atom of TCEP to generate the intermediate INTb with a free energy increase of 2.6 kcal/mol (Fig.4). The intermediate INTb decomposition is followed by the breaking of S–C bond with a barrier of 12.3 kcal/mol. After that, the sulfur atom of radical

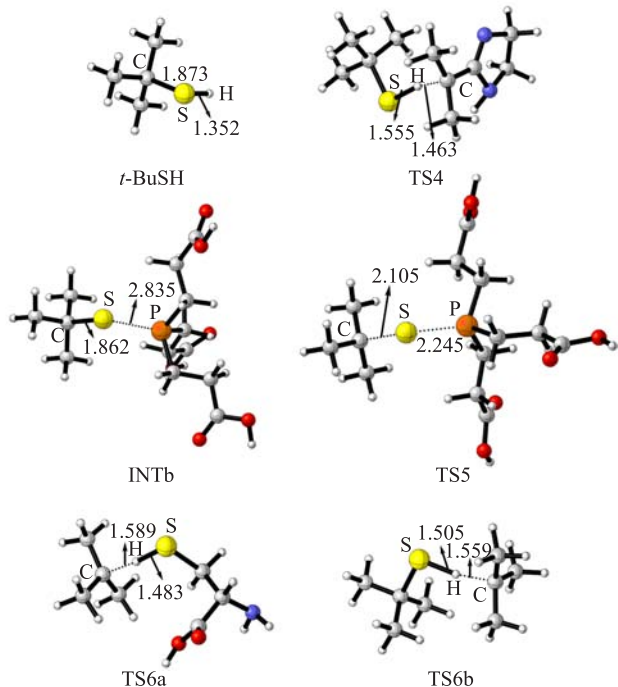


FIG. 4 Optimized geometries of species in the process of desulfurization of *t*-BuSH molecule. Bond length is in Å.

$R^2S\cdot$ is removed, accompanied with the formation of radical $R^2\cdot$.

The third step is the regeneration of RS· ($R=R^1$ or R^2). Similar to the radical $R^1\cdot$, the formed radical $R^2\cdot$ can either react with Cys to generate the active radical $R^1S\cdot$ via the hydrogen-transfer transition states TS6a, or react with *t*-BuSH to form radical $R^2S\cdot$ via TS6b. The relative free energies of TS6a and TS6b are 8.0 and 9.6 kcal/mol, respectively. Subsequently, both of

the formed radicals $R^1S\cdot$ and $R^2S\cdot$ can participate in the desulfurization cycle by reaction with TCEP (the second process of Fig.1 and Fig.3). The related calculation results shown in Fig.3 indicate that the regeneration of $R^1S\cdot$ is relatively more favorable (than that of $R^2S\cdot$) from both kinetic and thermodynamic aspects.

According to Fig.3, the rate-limiting step is the removal sulfur atom process, and the corresponding transition state is TS5 with a barrier of 14.9 kcal/mol.

D. The overall mechanism of the desulfurization in the concerned reaction system

For both of desulfurization pathways of R^1SH and R^2SH , the rate-limiting step is the desulfurization step. Comparing the detailed transformations in these two pathways, we can see that the hydrogen-abstraction process (the first step) involving Cys is relatively more facile than that involving *t*-BuSH. Meanwhile, the sulfur removal step involving *t*-BuSH is slightly more facile than the Cys pathway. Thereafter, the involvement of Cys in the third step (radical regeneration step) results in the regeneration of $R^1S\cdot$ radical. $R^1S\cdot$ represents the most stable intermediate in the reaction system, and it can be easily formed via the reaction of A with R^1SH . Therefore, the relative free energy of $R^1S\cdot$ determines the overall activation barrier of these two pathways. According to Fig.1 and Fig.3, the activation barriers of R^1SH pathway is 17.4 kcal/mol. By contrast, the R^2SH pathway has to first undergo the reverse reaction of hydrogen transfer step (from $R^1S\cdot$ to the starting point) to regenerate A. Therefore, the overall activation barrier of R^2SH pathway is 18.3 kcal/mol (the energy gap between $R^1S\cdot$ and TS4). In this context, the desulfurization of R^1SH is slightly more feasible. Nonetheless, the low energy difference between these two pathways indicates that they might be competitive. Interestingly, in the R^2SH pathway, *t*-BuSH is finally reduced to *t*-BuH with the generation of $R^1S\cdot$, which can then lead to the Cys pathway. Therefore, we suggest that the adduct *t*-BuSH facilitates the desulfurization of Cys by benefiting the formation of the requisite $R^1S\cdot$ in the R^1SH pathway. Finally, once all the Cys participate in the reaction system, the formed radical $R^1S\cdot$ will end the chain reaction by combining with each other (please see supplementary material for more details).

E. The mechanism of desulfurization in solution phase

To take the solvent effect into account [21], we also conducted solution-phase calculations in the present study. The modeling dipeptide compound R^3SH (used in Danishefsky's experiments) is used. In addition, considering that the zwitterionic forms of amino acids are more stable than their corresponding unionized forms in the solution phase [21(a), 22], we selected the zwitterionic form of R^3SH to examine its desulfurization mechanism.

The free energy profile of the R^3SH desulfurization process is shown in Fig.5. The geometries optimized in water are listed in Fig.S2 in supplementary material. Good consistency has been gained from the calculation results in solution and gas phases. For example, the relative free energies of all species in Fig.5 (the desulfurization mechanism of R^3SH) show the same trends as the gas phase calculation results (the desulfurization mechanism of Cys). That is, the desulfurization step is the rate determining step of the overall desulfurization process, and the radical regeneration step of cysteine residue is kinetically and thermodynamically more favorable than that of *t*-BuSH (TS9a vs. TS9b and $R^3S\cdot$ vs. $R^2S\cdot$). In addition, the optimized structures of each species in these two systems (gas phase and solution phase) are close to each other. For clarity, the optimized structures of TS8 and TS2 have been chosen as examples (Fig.6).

To better understand the driving force of the desulfurization process, we also calculated the C–SH and C–H bond dissociation energies (BDE) of R^1SH , R^2SH and R^3SH molecules (please see Table S1 in supplementary material for more details). The calculation results indicate that C–H BDEs are generally (96.1–105.4 kcal/mol) higher than the related C–SH BDEs (72.6–74.2 kcal/mol). Thus, the released energy by the formation of C–H bond somewhat compensates the energy demands in breaking the C–SH bond. This conclusion also explains the low energy barriers of the desulfurization step (<20 kcal/mol).

For comparison, the relative Gibbs free energies of the species in the gas phase and water solvent are listed in Table I. From Table I, it can be seen that the overall energy barrier in water (15.4 kcal/mol) is relatively lower than that of gas phase (17.4 kcal/mol). Therefore, it's expected that the selective desulfurization of Cys residue in water is more favorable than in gas phase (or low polar solvent). This proposal is verified by the natural population analysis (NPA) (Table S2 in the supplementary material). It's found that in the rate determining step (desulfurization step), the charge density on the carbon atom of the C–SH group gradually decreases, due to the interaction between the P atom of TCEP and the S atom of the $RS\cdot$ radical. The charge separation weakens the C–S bond, and thus facilitates the desulfurization step. Meanwhile, the charge of C atom in intermediate INTa is higher than that in INTc (-0.469 e vs. -0.452 e), indicating that the C–S bond strength of INTa is stronger than that of INTc, and the water solvent facilitates the desulfurization on R^3SH (relative to that on R^1SH). Finally, the low energy barriers in Fig.5 indicate that the reaction can be completed in a short time at room temperature. This conclusion is in good agreement with the experimental results of Danishefsky group [10].

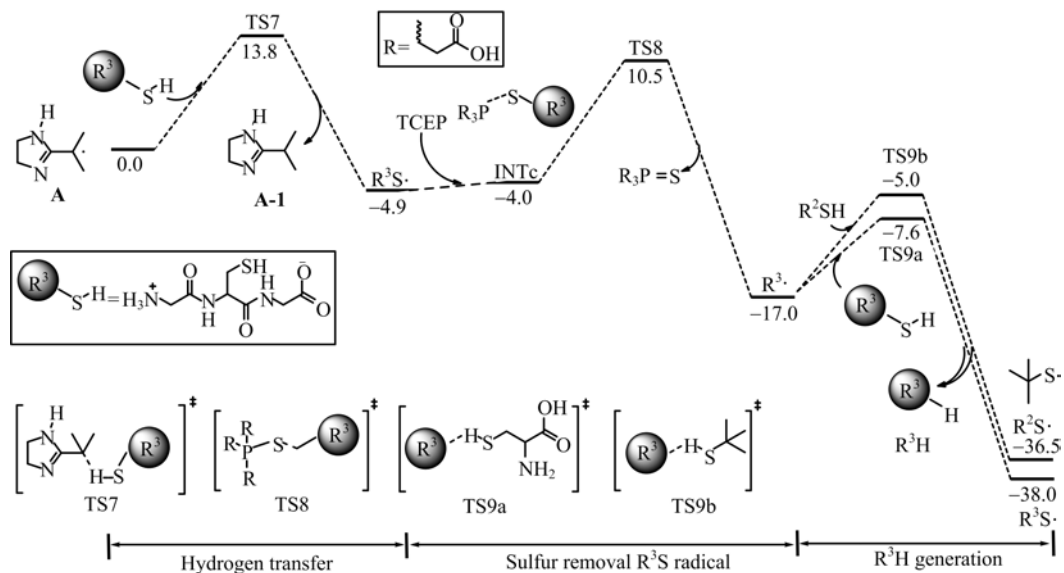


FIG. 5 Free energy profile of the desulfurization of R^3SH (in kcal/mol).

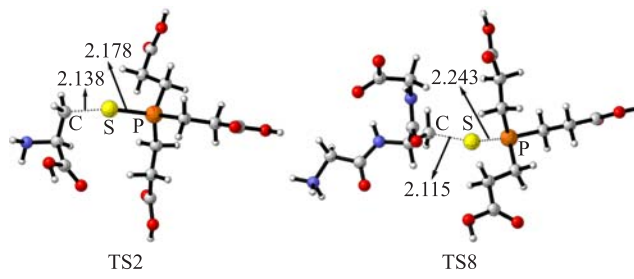


FIG. 6 Optimized geometries of transition state TS2 and TS8. Bond length is in Å.

IV. CONCLUSION

The mechanism of desulfurization of cysteine residue was studied using the density functional theory method. The calculated results show that the reactant undergoes hydrogen-transfer, removal of sulfur atom and regeneration of radical $\text{RS}\cdot$ processes subsequently. The rate-limiting step is the second step, *i.e.* removal of the sulfur atom via the reaction between radical of cysteine residue and the reductant (tris(2-carboxyethyl)phosphine in the present study). The adduct $t\text{-BuSH}$ molecule can facilitate the desulfurization because it helps the formation of cysteine residue radical (precursor of the desulfurization step).

Supplementary material: Termination process of desulfurization reaction, Optimized geometries of R^3SH desulfurization process, the BDE and NPA values of R^1SH , R^2SH and R^3SH molecules.

TABLE I The relative Gibbs free energies of the species involved in the desulfurization of cysteine in the gas phase and of R^3SH in water solvent, respectively.

	$\Delta G_{\text{gas}}/(\text{kcal/mol})$	$\Delta G_{\text{solv}}/(\text{kcal/mol})$	
A	0.0	0.0	
TS1	12.7	TS7	13.8
$\text{R}^1\text{S}\cdot$	-4.5	$\text{R}^3\text{S}\cdot$	-4.9
INTa	-1.3	INTc	-4.0
TS2	12.9	TS8	10.5
$\text{R}^1\cdot$	-10.4	$\text{R}^3\cdot$	-17.0
TS3a	-0.3	TS9a	-7.6
$\text{R}^1\text{S}\cdot$	-30.7	$\text{R}^3\text{S}\cdot$	-38.0
TS3b	1.7	TS9b	-5.0
$\text{R}^2\text{S}\cdot$	-28.8	$\text{R}^2\text{S}\cdot$	-36.5

V. ACKNOWLEDGMENTS

This work was supported by the National Natural Science Foundation of China (No.21202006), the Fundamental Research Funds for the Central Universities of Ministry of Education of China (No.FRF-TP-14-015A2), the Natural Science Foundation of Anhui Province (No.1308085QB38), and the Supercomputer Centre of Shanghai.

[1] P. E. Dawson, T. W. Muir, L. C. Lewis, and S. B. H. Kent, *Science* **266**, 776 (1994).

[2] (a) J. Chen, G. Chen, B. Wu, Q. Wan, Z. Tan, Z. Hua, and S. J. Danishefsky, *Tetrahedron Lett.* **47**, 8013 (2006).
 (b) R. K. McGinty, J. Kim, C. Chatterjee, R. G. Roeder, and T. W. Muir, *Nature* **453**, 812 (2008).
 (c) G. M. Fang, Y. M. Li, F. Shen, Y. C. Huang, J. B. Li, Y. Lin, H. K. Cui, and L. Liu, *Angew. Chem. Int. Ed.* **50**, 7645 (2011).
 (d) P. E. Dawson and S. B. H. Kent, *Annu. Rev. Biochem.* **69**, 923 (2000).
 (e) J. S. Zheng, S. Tang, Y. C. Huang, and L. Liu, *Acc. Chem. Res.* **46**, 2475 (2013).
 (f) K. S. Kumar, S. N. Bavikar, L. Spasser, T. Moyal, S. Ohayon, and A. Brik, *Angew. Chem. Int. Ed.* **50**, 6137 (2011).
 (g) Y. M. Li, Y. T. Li, M. Pan, X. Q. Kong, Y. C. Huang, Z. Y. Hong, and L. Liu, *Angew. Chem. Int. Ed.* **53**, 2198 (2014).
 (h) C. Mayer, M. M. Mueller, S. H. Gellman, and D. Hilvert, *Angew. Chem. Int. Ed.* **53**, 6978 (2014).

[3] (a) S. B. H. Kent, *Chem. Soc. Rev.* **38**, 338 (2009).
 (b) V. Y. Torbeev and S. B. H. Kent, *Angew. Chem. Int. Ed.* **46**, 1667 (2007).
 (c) Y. Sohma and S. B. H. Kent, *J. Am. Chem. Soc.* **131**, 16313 (2009).
 (d) D. Bang, B. L. Pentelute, and S. B. H. Kent, *Angew. Chem. Int. Ed.* **45**, 3985 (2006).
 (e) K. Mandal and S. B. H. Kent, *Angew. Chem. Int. Ed.* **50**, 8029 (2011).
 (f) G. M. Fang, J. X. Wang, and L. Liu, *Angew. Chem. Int. Ed.* **51**, 10347 (2012).
 (g) Y. C. Huang, Y. M. Li, Y. Chen, M. Pan, Y. T. Li, L. Yu, Q. X. Guo, and L. Liu, *Angew. Chem. Int. Ed.* **52**, 4858 (2013).
 (h) M. T. Weinstock, M. T. Jacobsen, and M. S. Kay, *Proc. Natl. Acad. Sci. USA* **111**, 11679 (2014).

[4] (a) B. Wu, J. Chen, J. D. Warren, G. Chen, Z. Hua, and S. J. Danishefsky, *Angew. Chem. Int. Ed.* **45**, 4116 (2006).
 (b) L. E. Canne, S. J. Bark, and S. B. H. Kent, *J. Am. Chem. Soc.* **118**, 5891 (1996).
 (c) R. Kleineweischede and C. P. R. Hackenberger, *Angew. Chem. Int. Ed.* **47**, 5984 (2008).
 (d) G. Chen, Q. Wan, Z. Tan, C. Kan, Z. Hua, K. Ranganathan, and S. J. Danishefsky, *Angew. Chem. Int. Ed.* **46**, 7383 (2007).
 (e) R. J. Hondal, B. L. Nilsson, and R. T. Raines, *J. Am. Chem. Soc.* **123**, 5140 (2001).
 (f) J. Offer, C. N. C. Boddy, and P. E. Dawson, *J. Am. Chem. Soc.* **124**, 4642 (2002).
 (g) N. Metanis, E. Keinan, and P. E. Dawson, *Angew. Chem. Int. Ed.* **49**, 7049 (2010).
 (h) J. S. Zheng, S. Tang, Y. K. Qi, Z. P. Wang, and L. Liu, *Nature Protocols* **8**, 2483 (2013).
 (i) J. X. Wang, G. M. Fang, Y. He, D. L. Qu, M. Yu, Z. Y. Hong, and L. Liu, *Angew. Chem. Int. Ed.* **54**, 2194 (2015).
 (j) R. E. Thompson, X. Y. Liu, N. Alonso-Garcia, P. J. B. Pereira, K. A. Jolliffe, and R. J. Payne, *J. Am. Chem. Soc.* **136**, 8161 (2014).

[5] L. Z. Yan and P. E. Dawson, *J. Am. Chem. Soc.* **123**, 526 (2001).

[6] (a) D. Crich and A. Banerjee, *J. Am. Chem. Soc.* **129**, 10064 (2007).
 (b) B. L. Pentelute and S. B. H. Kent, *Org. Lett.* **9**, 687 (2007).
 (c) D. Bang, G. I. Makhadze, V. Tereshko, A. A. Kossiakoff, and S. B. H. Kent, *Angew. Chem. Int. Ed.* **44**, 3852 (2005).
 (d) J. S. Zheng, H. N. Chang, F. L. Wang, and L. Liu, *J. Am. Chem. Soc.* **133**, 11080 (2011).

[7] E. C. B. Johnson, E. Malito, Y. Shen, D. Rich, W. Tang, and S. B. H. Kent, *J. Am. Chem. Soc.* **129**, 11480 (2007).

[8] M. B. Smith, *J. March, March's Advanced Organic Chemistry-Reactions, Mechanisms, and Structure*, 6th Edn., Hoboken: Wiley, 848 (2007).

[9] (a) K. Nishide, Y. Shigeta, K. Obata, T. Inoue, and M. Node, *Tetrahedron Lett.* **37**, 2271 (1996).
 (b) M. Node, K. Nishide, Y. Shigeta, K. Obata, H. Shiraki, and H. Kunishige, *Tetrahedron* **53**, 12883 (1997).

[10] Q. Wan and S. J. Danishefsky, *Angew. Chem. Int. Ed.* **46**, 9248 (2007).

[11] (a) C. Haase, H. Rohde, and O. Seitz, *Angew. Chem. Int. Ed.* **47**, 6807 (2008).
 (b) P. W. R. Harris and M. A. Brimble, *Int. J. Pept. Res. Ther.* **18**, 63 (2012).
 (c) Q. Q. He, G. M. Fang, and L. Liu, *Chin. Chem. Lett.* **24**, 265 (2013).

[12] F. W. Hoffmann, R. J. Ess, T. C. Simmons, and R. S. Hanzel, *J. Am. Chem. Soc.* **78**, 6414 (1956).

[13] (a) C. Walling and R. Rabinowitz, *J. Am. Chem. Soc.* **79**, 5326 (1957).
 (b) C. Walling, O. H. Basedow, and E. S. Savas, *J. Am. Chem. Soc.* **82**, 2181 (1960).

[14] M. J. Frisch, G. W. Trucks, H. B. Schlegel, G. E. Scusearia, M. A. Robb, J. R. Cheeseman, G. Scalmani, V. Barone, B. Mennucci, G. A. Petersson, H. Nakatsuji, M. Caricato, X. Li, H. P. Hratchian, A. F. Izmaylov, J. Bloino, G. Zheng, J. L. Sonnenberg, M. Hada, M. Ehara, K. Toyota, R. Fukuda, J. Hasegawa, M. Ishida, T. Nakajima, Y. Honda, O. Kitao, H. Nakai, T. Vreven, J. A. Jr. Montgomery, J. E. Peralta, F. Ogliaro, M. Bearpark, J. J. Heyd, E. Brothers, K. N. Kudin, V. N. Staroverov, T. Keith, R. Kobayashi, J. Normand, K. Raghavachari, A. Rendell, J. C. Burant, S. S. Iyengar, J. Tomasi, M. Cossi, N. Rega, J. M. Millam, M. Klene, J. E. Knox, J. B. Cross, V. Bakken, C. Adamo, J. Jaramillo, R. Gomperts, R. E. Stratmann, O. Yazyev, A. J. Austin, R. Cammi, C. Pomelli, J. W. Ochterski, R. L. Martin, K. Morokuma, V. G. Zakrzewski, G. A. Voth, P. Salvador, J. J. Dannenberg, S. Dapprich, A. D. Daniels, Ö. Farkas, J. B. Foresman, J. V. Ortiz, J. Cioslowski, and D. J. Fox, *Gaussian 09, Revision D.01*, Wallingford CT: Gaussian, Inc., (2013).

[15] (a) K. Fukui, *J. Phys. Chem.* **74**, 4161 (1970).
 (b) K. Fukui, *Acc. Chem. Res.* **14**, 363 (1981).
 (c) H. P. Hratchian and H. B. Schlegel, *J. Chem. Phys.* **120**, 9918 (2004).

[16] (a) Y. Zhao and D. G. Truhlar, *Theor. Chem. Acc.* **120**, 215 (2008).
 (b) Y. Zhao and D. G. Truhlar, *Acc. Chem. Res.* **41**, 157 (2008).
 (c) H. J. Xie, W. S. Mou, F. R. Lin, J. H. Xu, Q. F. Lei, and W. J. Fang, *Acta Phys.-Chim. Sin.* **29**, 1421 (2013).

(d) E. Dames, B. Sirjean, and H. Wang, *J. Phys. Chem. A* **114**, 1161 (2010).
(e) P. A. J. Denis, *Comput. Chem.* **17**, 1511 (2012).
(f) O. Karahan, V. Aviyente, D. Avci, H. Zijlstra, and F. M. J. Bichelhaupt, *J. Polym. Sci., Part A* **51**, 880 (2013).

[17] A. V. Marenich, C. J. Cramer, and D. G. Truhlar, *J. Phys. Chem. B* **113**, 6378 (2009).

[18] (a) S. Cheng, S. R. S. Ting, F. P. Lucien, and P. B. Zetterlund, *Macromolecules* **45**, 1803 (2012).
(b) W. M. Gramlich, J. L. Holloway, R. Rai, and J. A. Burdick, *Nanotechnology* **25**, 14004 (2014).
(c) H. Nambu, K. Hata, M. Matsugi, and Y. T. Kita, *Chem. Commun.* 1082 (2002).

[19] (a) J. Qiu, S. G. Gaynor, and K. Matyjaszewski, *Macromolecules* **32**, 2872 (1999).
(b) M. Li and K. Matyjaszewski, *Macromolecules* **36**, 6028 (2003).
(c) H. Nambu, K. Hata, M. Matsugi, and Y. Kita, *Chem. Eur. J.* **11**, 719 (2005).

[20] (a) A. SchJnberg, *Ber. Dtsch. Chem. Ges.* **68**, 163 (1935).
(b) J. A. Burns, J. C. Butler, J. Moran, and G. M. Whitesides, *J. Org. Chem.* **56**, 2648 (1991).
(c) J. C. Han and G. Y. Han, *Anal. Biochem.* **220**, 5 (1994).
(d) E. B. Getz, M. Xiao, T. Chakrabarty, R. Cooke, and P. R. Selvin, *Anal. Biochem.* **273**, 73 (1999).

[21] (a) C. Wang, Q. X. Guo, and Y. Fu, *Chem. Asian J.* **6**, 1241 (2011).
(b) C. Wang and Q. X. Guo, *Sci. China Chem.* **55**, 2075 (2012).
(c) C. Wang, H. Z. Yu, Y. Fu, and Q. X. Guo, *Org. Biomol. Chem.* **11**, 2140 (2013).

[22] Q. Zhang, H. Z. Yu, and J. Shi, *Acta Phys. -Chim. Sin.* **29**, 2321 (2013).